

# Biosynthesis of zinc oxide nanoparticles by hot aqueous extract of *Allium sativum* plants

Dhuha Kadhem Slman\*, Raghad Dhyea Abdul Jalill\*, Ahmed N. Abd\*\*

\*Department of Biology/ College of Science/ Mustainsiriyah University/ Baghdad /Iraq.

\*\*Department of Physics/ College of Science, Mustainsiriyah University, Baghdad, Iraq.

## Abstract

Current studies interested on the biosynthesis of zinc oxide nanoparticles (ZnO-NPs) using hot plants extracts of *Allium sativum* and characterization of them using: Atomic Force Microscopy (AFM), X-ray diffractions (XRD), Fourier Transform Infrared Spectroscopy (FT-IR), UV-visible spectral and Hot stage.

The results found that all NPs are had nano-size. ZnO NPs was produced by four procedures using hot extract of *Allium sativum*. The average diameters were: 101.59 nm, 110.33 nm, 75.69 nm, 88.67 nm for first, second, third and fourth procedures respectively compared with 47.57 nm for standard NPs. The Roughness averages (Ra) were: 10.8 nm, 6.83 nm, 13.8 nm, 0.541 nm for first, second, third and fourth respectively. The Root mean square (Sq) were: 12.8 nm, 8.68 nm, 16 nm, 0.673 nm for first, second, third and fourth respectively. Their averages crystallites was determine using Scherer's equation, they were: (41.489, 42.125, 45.593 and 46.375) nm respectively compared with 79.505 nm for standard NPs.

**Keyword:** *Allium sativum*; plant; synthesis, ZnO-NPs.

## INTRODUCTION

Nanotechnology include the usage and production of material at nanoscale dimensions less than one hundred nanometres (1). These provide NPs large surface area to volume ratio. ZnO-NPs showed huge semiconducting properties due to its high exciton binding energy (60 meV) and they have large band gap (3.37 eV) (2); (3). They exhibits high catalytic efficiency, strong adsorption ability, optic and UV filtering properties (4); (5).

They have vast applications such as optical, piezoelectric, gas sensing and magnetic. Besides, they are used some industries products such as: ceramics, sunscreens and rubber, wastewater treatment, and as a fungicide 7).

It has various pharmaceutical applications, (7) such as: drug delivery, anti-cancer, modulating allergic reactions via inhibition of mast cell degranulation, anti-diabetic, antibacterial activity (8), (9), anti-fungal and agricultural properties. cell imaging (10).

These NPs could be fabricate by different chemical and physical procedures which may prove hazardous in the field of their application in the medical field (11). Physical procedures includes high vacuum, high temperature for examples: pulsed laser deposition, thermal evaporation, molecular beam epitaxy (MBE), etc.. (12). Chemical procedures include: micro emulsion, wet chemical, spray pyrolysis, electrode- position (12). These approach is an environment-friendly, cost- effective, biocompatible, safe, green approach (13) and they allow large scale production of pure ZnO-NPs without any impurity (14) .

There were various plant extracts od different plant which could use for synthesis ZnO NPs, (15) , including fresh or dry: leaves, rhizome, flower and fruit (16). ZnO-NPs could produce by sodium hydroxide and zinc acetate which found in of leaves of *Catharanthus roseus*.

Aqueous dispersed zinc nanoparticles (Zn-NPs) were synthesized using either natural polysaccherides such as chitosan, alginate and citrus pectin which isolated from *Pleurotus ostreatus* as reducing or stabilizing agent with the average size is 46 nm (17).

Garlic (*Allium sativum*)/ Liliaceae family, is among the oldest of all cultivated plants because of its medical properties (18), (19).

The ultimate bioactive compound of garlic is organo-sulfure components, i.e. alliin, allicin, ajoene, allyl sulphide groups, and allyl cysteine(20), and other compounds such as: flavonoids, fatty acids, amino acids, glycolipids, vitamins phospholipids, phenolics and (21), vitamin C and phenolic compounds (19). The extraction of *A. sativum* plant mediated silver nano particles (22). Ethanollic plant extracts of garlic could use to synthesis tetragonal and hexagonal forms zinc nanoparticles with size range of 99.34–134.57 nm, (23). This study aims to biosynthesis of ZnO-NPs by hot extracts of bulbs of *Allium sativum* plants with the characterization of nanoparticles.

## MATERIALS AND METHODS

### 1. Plant extraction:

Fleshy Bulbs of *Allium sativum* were used for synthesis, it obtained from Iraqi local markets and identified in the Herbarium of Iraqi Ministry of Health. Fifteen grams of Bulbs mixed with 250 ml of distal water by homogenized blender either for four minutes, then, the mixture putted in hot stone at 50 °C for 5 hours and this is called hot extracts. They filtered by Whatman 4 filter paper. The residue was cast away. The filtrate utilized for the biosynthetic of NPs immediately.

### 2. Synthesis

This is done by methods that appeared in table (1) which optimized: the final concentrations of plant extracts and bulk particles, temperature and exposure time. Separately, plant extract was mixed with bulk particles in flask, placed in magnetic steer hot plate at various tempters with 1000 rpm /second for different exposure time. The solutions allowed to cool at room temperature and repeated centrifugations at 15,000 rpm for ten minute. The supernatant is neglected. The precipitates was washed using double distilled water thence centrifuged at 1500 rpm for ten minute. This is repeated three times. The obtained precipitate dried at room temperature for 24 h. and characterized.

Table (1): Conditions of Biosynthetic of ZnO-NPs by some plant extracts.

Plant extracts	procedures	P.EX.(ml)	BPs(mg/ml)	T.(C°)	Exp.(hr.)
Hot	1	100	5	75	10
	2	100	5	50	10
	3	50	10	75	10
	4	50	10	50	12

P.EX.: Quantities of plant extracts; BPs: bulk particles T.: temperature (C°) and Exp.: exposure time (hr.).

### 3. CHARACTERIZATION

The techniques, which used for characterization nanoparticles, were: **Atomic Force Microscopy (AFM)**, (Shimadzu-Japan/AA3000), (24), **X-ray diffractions (XRD)** (Shemadzu/ Japan) was used to affirm the crystal phases and size. It was carry out using X-ray diffractometer with Cu-K $\alpha$  crystal radiation ( $\lambda = 1.541 \text{ \AA}$ ) scanning at a rate of ( $5^\circ/\text{min}^{-1}$ ) for (2theta) range of ( $5^\circ - 80^\circ$ ). The diffraction peaks were identified by comparison with (00-036-1451) card/ Variable Slit Intensity. The full widths at half maximum (FWHM) in the XRD was used to determine the crystallite size by Scherer's equation, (25), The strain values  $\eta$ , (26), and the values of dislocation densities  $\delta$ , (27), were, calculated. **Fourier Transform Infrared Spectroscopy (FT-IR)**, Shemadzu, (Germany), spectrum was also used, The peaks, in FT-IR, correspond to the Zn-O stretching vibrations according to NIST WEB BOOK, (<http://webbook.nist.gov/>).. **UV-visible spectrum** (Schimadzu 1601 spectrophotometer) in 250–900 nm range, (28). Transmittance measurements, absorption coefficient and the gap energy were calculated for optical properties as described by Meshram and others in (2012). **Hot stage microscope (HSM)**/ Vega Tescan (USA) was also used for

characterization the thermal behavior of the ZnO nanoparticles, the samples were visually examined by deposited on a glass substrates at 25°C according to a Drop Casting Method. Microscopic observations during experiments were displayed on a computer screen and recorded using a JVC color video camera, (29).

## RESULTS AND DISCUSSION

### 1. Hot extracts

**Atomic force microscopy:** The average diameters were: 101.59 nm, 110.33 nm, 75.69 nm, 88.67 nm for first, second, third and fourth procedures respectively compared with 47.57 nm for standard NPs. Figure (1) showed the granularity volume distribution chart for all ZnO NPs. The Roughness averages (Ra) were: 10.8 nm, 6.83 nm, 13.8 nm, 0.541 nm for first, second, third and fourth procedures respectively compared with 0.827 nm for standard NPs. The Root mean squares (Sq) were: 12.8 nm, 8.68 nm, 16 nm, 0.673 nm for first, second, third and fourth procedures respectively compared with 0.999 nm for standard NPs.. Figure (2) showed AFM topographic images of biosynthesis ZnO nanoparticles.

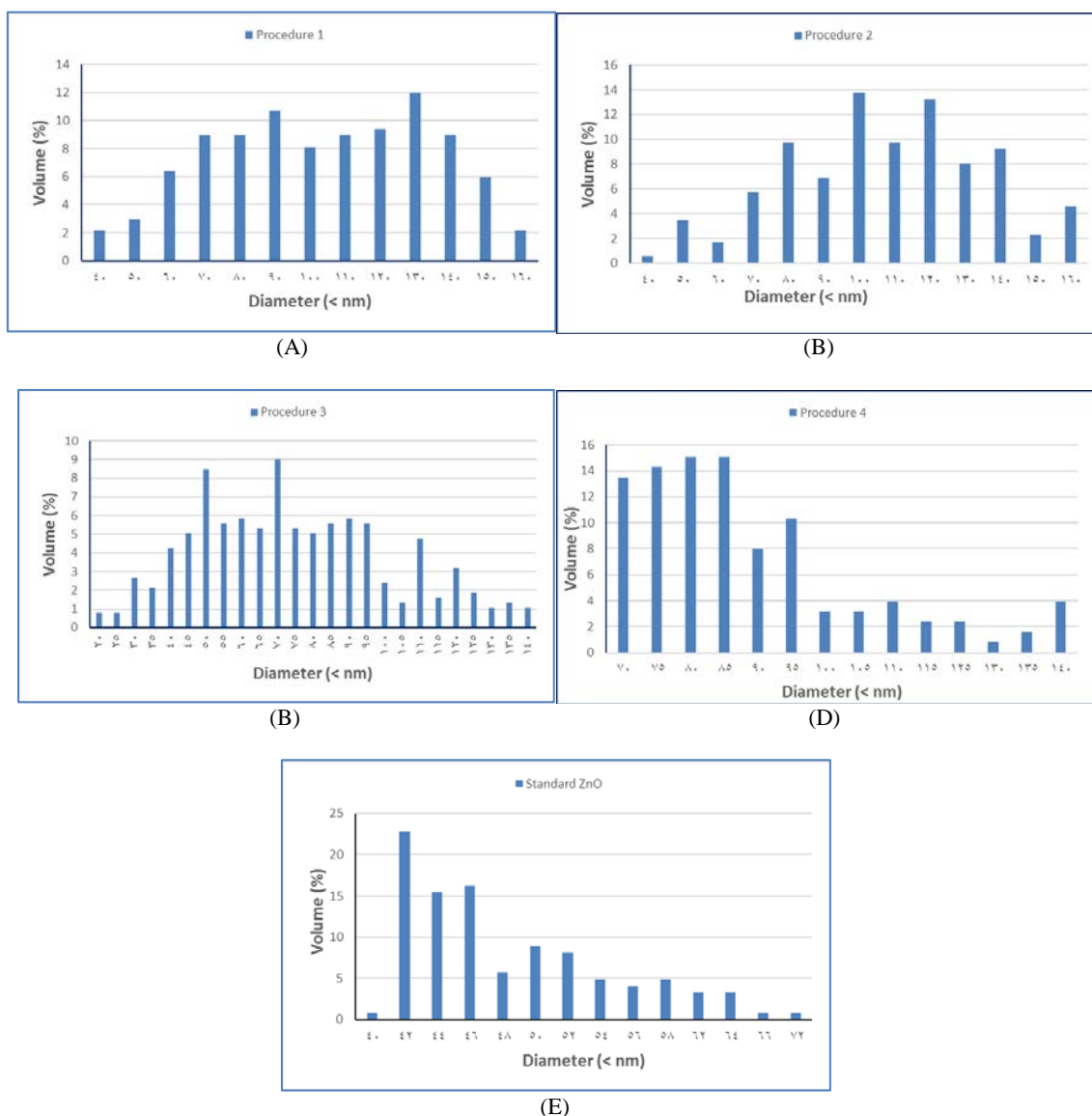


Fig. (1): Granularity volume distribution chart of ZnO NPs produced by *A. sativum* hot extracts using: (A) first, (B) second, (C) third, (D) fourth procedures, respectively and (E) standard NPs.

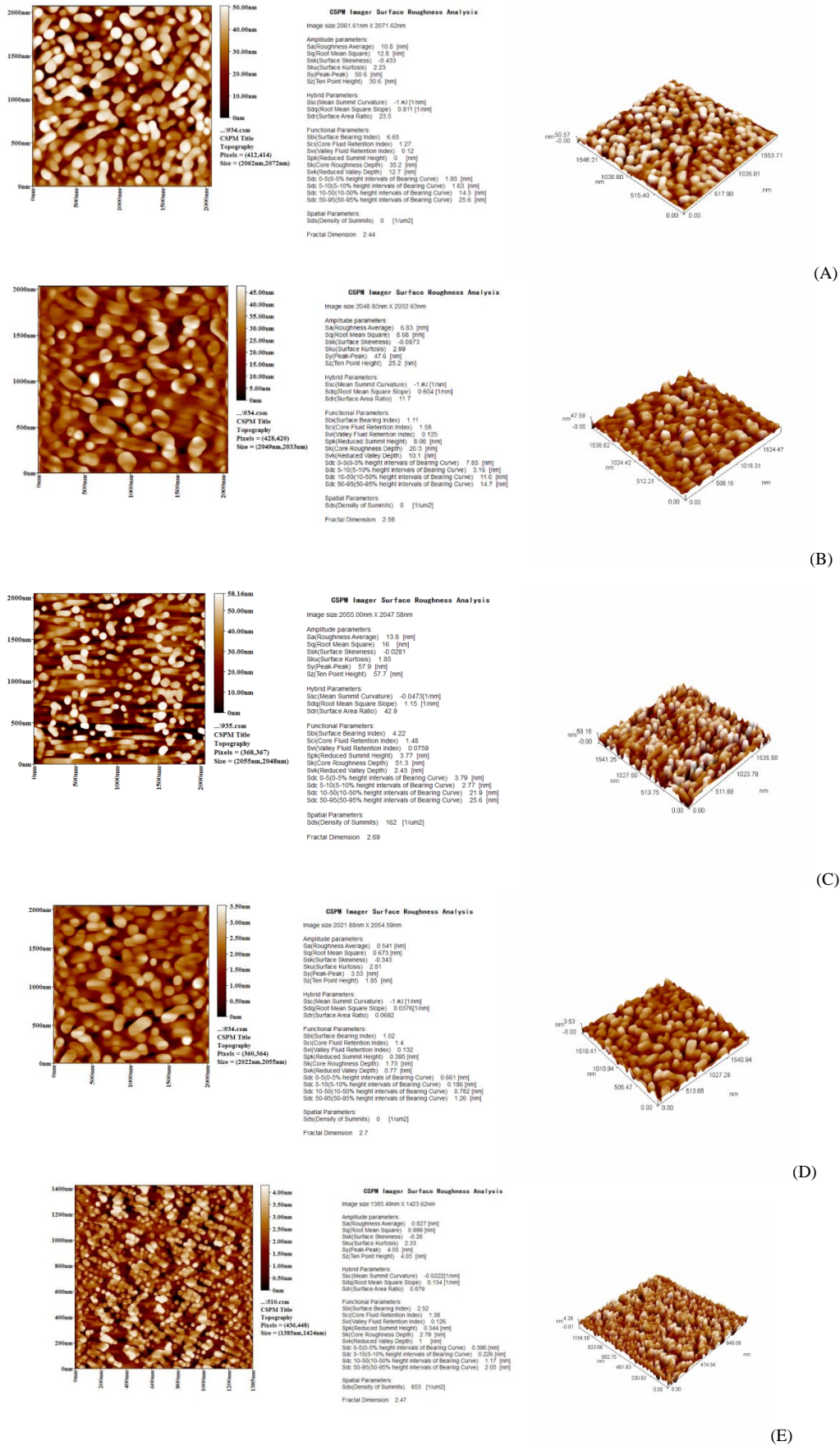


Fig. (2): AFM topographic of ZnO-NPs fabricated by *A. sativum* hot extracts using: (A) first, (B) second, (C) third, (D) fourth procedures, respectively and (E) standard NPs.

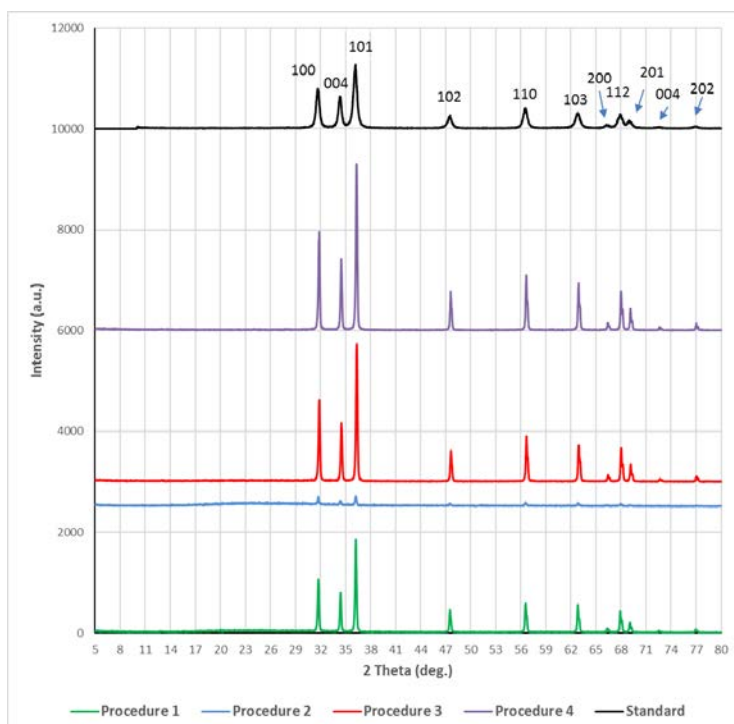


Fig. (3): X-Ray patterns of ZnO NPs synthesis by *A. sativum* hot plant extract, data showed procedure 1, 2, 3, 4 compared with standard NPs.

Table (2): summary of X-ray characterizations of ZnO-NPs biosynthesis nanoparticles synthesis by *A. sativum* hot plant extract.

Sample	Planes (hkl)	2 theta (DEG)	FWHM (DEG)	D (nm)	STRAIN XE-4	DIS X1014
Procedure 1	101	36.263	0.198	41.965	33.028	5.678
	100	31.779	0.196	41.840	33.126	5.712
	002	34.435	0.204	40.663	34.085	6.048
Procedure 2	101	36.204	0.208	39.943	34.700	6.268
	100	31.712	0.172	47.823	28.982	4.372
	002	34.381	0.214	38.608	35.900	6.709
Procedure 3	101	36.361	0.188	44.231	31.336	5.111
	100	31.878	0.179	46.047	30.099	4.716
	002	34.534	0.178	46.500	29.806	4.625
Procedure 4	101	36.342	0.177	47.055	29.455	4.516
	100	31.858	0.184	44.693	31.012	5.006
	002	34.513	0.175	47.376	29.255	4.455
Standard	101	36.173	0.510	84.940	37.558	16.317
	100	31.696	0.471	79.425	32.838	17.451
	002	34.355	0.443	74.150	28.622	18.692

(hkl) planes: crystallographic plane; FWHM: Full width at half maximum; D: dimension of Crystal in nm;  $\eta \times 10^{-4}$ : strain value;  $\delta \times 10^{14}$ : dislocation density; NPs: nanoparticles.

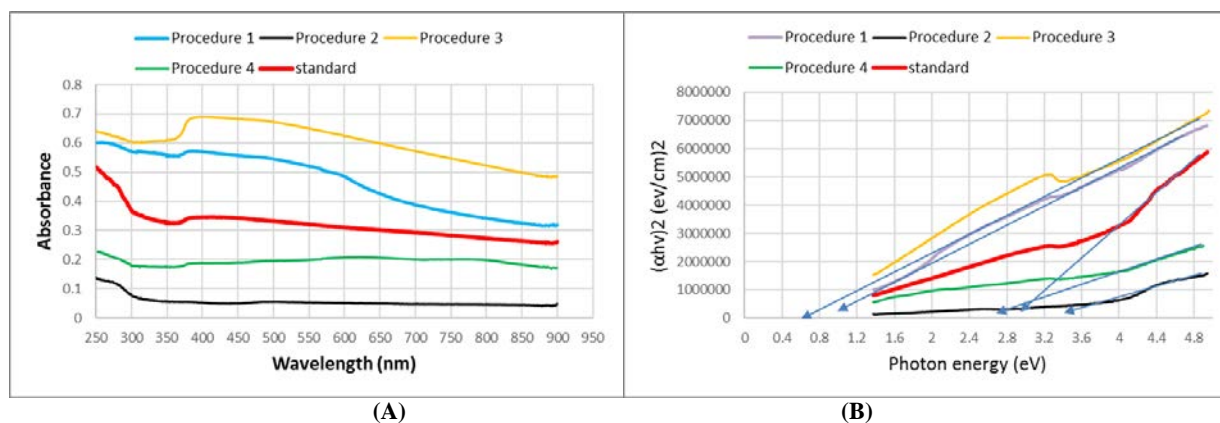


Fig. (4): (A) absorptions spectrum and (B)  $(ahv)^2$  versus photon energy of biosynthetic ZnO NPs using *A. sativum* hot plant extracts, data showed procedure 1, 2, 3, 4 compared with standard NPs.

**X-ray diffraction:** There were eleven peaks in each XRD pattern of NPs produced by *A. sativum* hot extracts and strong diffraction peaks are: 31.7 (100), 34.42 (002), 36.2 (101), 47.54 (102), 56.64 (110), 62.58 (103), 66.24 (200), 67.92 (112), 69.06 (201), 72.62 (004), 76.9 (202), (Figure 3). Their averages crystallites size were: 41.5 nm, 42.1 nm, 45.6 nm and 46.4 nm for procedure 1, 2, 3 and 4 respectively. It was notice that averages crystallites size of all of these biosynthetic nanoparticles were smaller than stander nanoparticles averages 79.5 nm. Their strain values and dislocation densities were found in Table (2).

**UV-visible spectral:** The absorption spectral of biosynthesis ZnO-NPs demonstrated strong absorption at 400 nm for the first procedure while it was 250 for each of second, third and fourth biosynthesis NPs in addition to standard NPs, Figure (4 A). The values of optical band gaps were: 1.35 eV and 3.6 eV for first and second procedures respectively, and they were 1.1 eV and 3.05 eV for third and fourth procedures respectively, compared with 3 eV for standard NPs Figure (4 B).

The high energy gap of ZnO-NPs which fabricate by second procedure (3.6 eV) compared with commercial ZnO (3 eV) in current study might due to the large amount of plant extracts and moderate temperature in the reaction compared with other procedures which (had low energy gaps in current results) this may be due to either low quantities of plant extract (not enough to reducing the ions) or high temperatures of reactions which may damage the compounds in plant extract that might acts as reducing agents. In the other hand the physio-chemical method of Kakil in (2014) found that ZnO NPs has direct band gap energy of 3.37 eV.

**FTIR:** The finding of Figure (5), showed fundamental mode of vibration at 640 cm<sup>-1</sup>, 1004 cm<sup>-1</sup>, 1086 cm<sup>-1</sup> and 1649 cm<sup>-1</sup> for standard NPs which correspond to the Zn-O stretching vibration. The Zn-O stretching vibration of biosynthetic NPs observed at: 640 cm<sup>-1</sup>, 1004 cm<sup>-1</sup>, 1086 cm<sup>-1</sup> and 1649 cm<sup>-1</sup> for first procedure, 611 cm<sup>-1</sup>, 1004 cm<sup>-1</sup>, 1086 cm<sup>-1</sup> and 1645 cm<sup>-1</sup> for second procedure, 609 cm<sup>-1</sup>, 1004 cm<sup>-1</sup>, 1086 cm<sup>-1</sup> and 1645 cm<sup>-1</sup> for third procedure, 640 cm<sup>-1</sup>, 1004 cm<sup>-1</sup>, 1086 cm<sup>-1</sup> and 1656 cm<sup>-1</sup> for fourth procedure, all of these peaks correspond to the Zn-O stretching vibration according to NIST WEB BOOK, (<http://webbook.nist.gov/>).

**Hot stage:**

Figure (6 A) is a microscopic image of the first method deposited on a glass substrate at room temperature (As-prepared) in a Drop Casting Method. The particles of ZnO thin films have been noticed as that the particles are aggregate in different diameters, semispherical (ball shape) and constriction with the nanostructure particles. Figure (6 B) was a microscopic image which was prepared by the second method indicate that the particles arranged as large orange aggregations and wide distributed on a glass to form a nano structure. Figure (6 C), prepared by third method, found that the particles arranged as twins black aggregations. Figure (6 D) microscopic image of NPs fabricated by fourth method found the particles was arranged as high brown aggregations to form nanostructure particles. Figure (6 E) is the microscopic image of standard ZnO showed that the particles constructed as a high concentrations with different diameters and take semis-spherical shapes as a nanostructure.

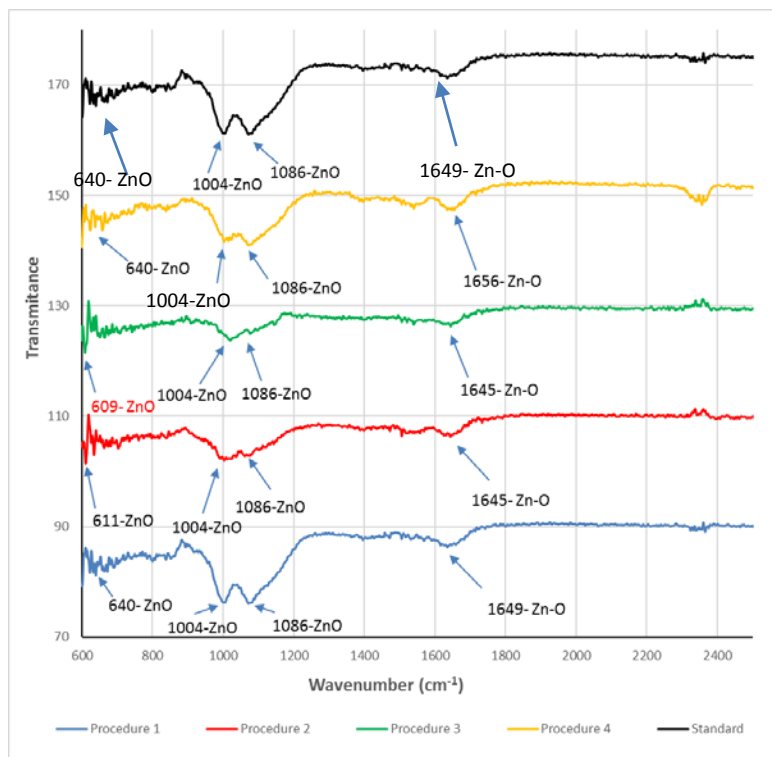


Fig. (5): FT-IR spectra of ZnO NPs synthesis by *A. sativum* hot plant extract, data showed procedure 1, 2, 3, 4 compared with standard NPs.

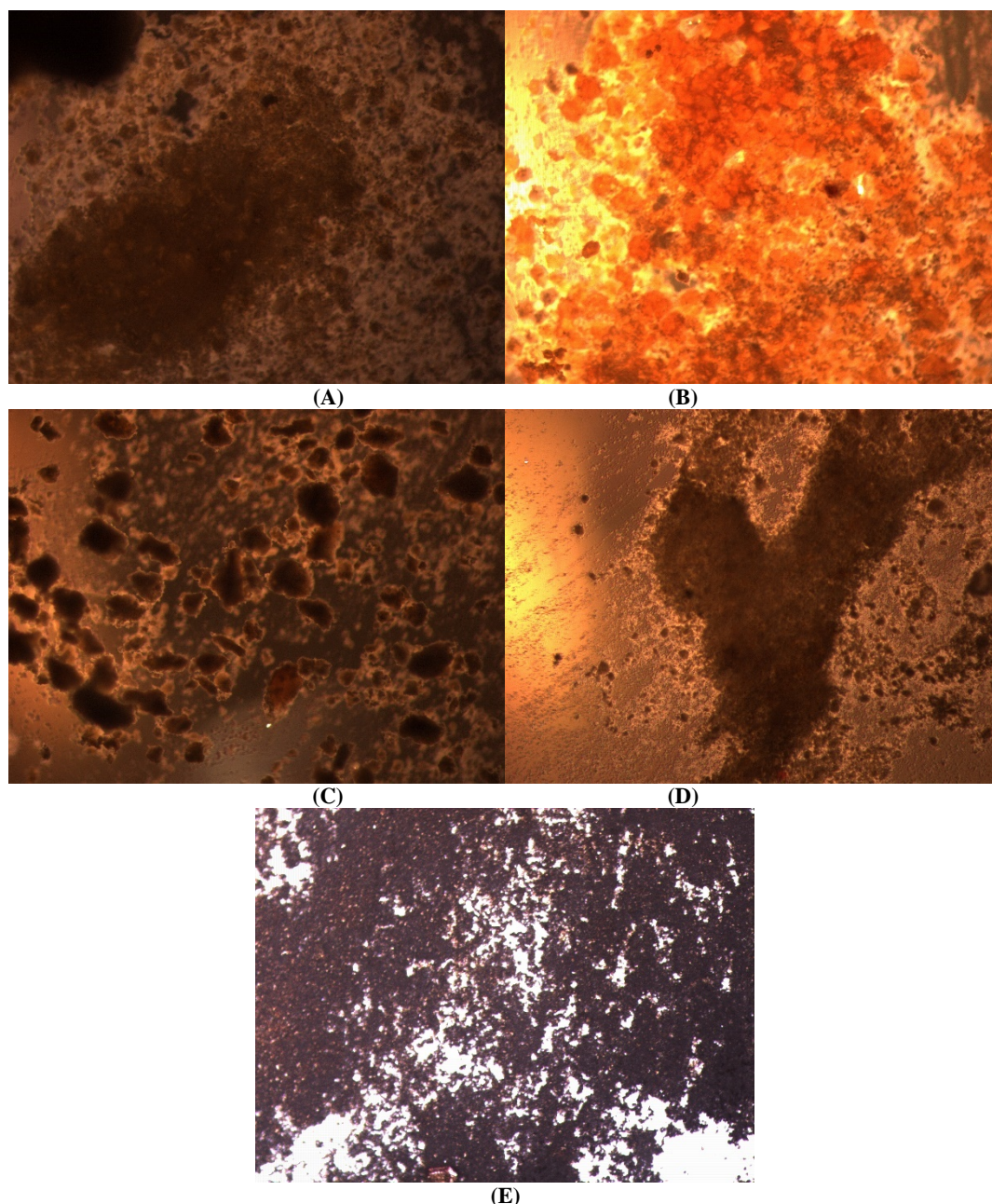


Fig. (6): Hot stage of ZnO NPs using *A. sativum* hot plant extract, data showed: (A) first, (B) second, (C) third, (D) fourth compared with (E) standard NPs.

In current study, hot extracts of *A. sativum* plant were successfully fabricate ZnO nanoparticles by four procedure these include variation in concentrations of a plant extracts, concentrations of bulk particles and temperature. When the concentrations of a plant extract were decrease and the concentrations of bulk particles were increased, the sizes of synthesized ZnO-NPs were decrease. Results also compared the size ranges observed through different techniques like AEM and XRD which showed different range values.

Garlic contain various compounds such as: flavonoids, fatty acids, amino acids, phospholipids, glycolipids, phenolics, and vitamins (21), saturated fatty acids: Capric acid, Caproic acid, Lauric acid, Myristic acid and Palmitic acid, Heptadecanoic acid, Stearic acid, Heneicosanoic acid, Tricosanoic acid, Lignoceric acid in addition to Unsaturated fatty acids: Palmitoleic acid, Oleic acid, Linoleic acid, Linolenic Acid and Arachidonic acid (30). In addition to

vitamin C, phenol, alliin, flavonoid, gallic, catechin hydrate, (19) and various polysaccharides.

Phytochemicals present in the garlic might responsible for the quick reduction of Zn bulk particles to nanoparticles in a single step eco-friendly processing. Polysaccharides, which have hydroxyl groups and hemiacetal reducing ends could play prominent roles in reduction metallic nanoparticles, (31). The reducing agents of garlic may involve the various compounds in plant such as phenolic, alkaloids, terpenoids and co-enzymes, (32). Recently, some studies approved the activity of pure compound in fabrication of ZnO NP, for examples: Egg albumin could synthesis were Spherical and Hexagonal ZnO NP with 16 nm (XRD) and 10–20 nm (TEM), 8–22 nm (AFM), starch 50 nm (SEM) (33), and L-alanine 50–110 nm (TEM, SEM), (34), could , also produced ZnO NP.

## CONCLUSIONS

Hot extracts of *A. sativum* plant were successfully fabricate ZnO nanoparticles. More studies about the role of garlic primary and secondary compounds in the fabricate ZnO nanoparticles will be beneficial.

## Acknowledgments

The authors would like to thank Mustainsiriyah University (www.uomustainsiriyah.edu.iq) Baghdad Iraq for its support in the present work.

## REFERENCES

- Kelsall, R.W.; Hamley, I.W. and Geoghegan, M. (2005). Nanoscale science and technology. John Wiley and Sons Ltd. 473.
- Elumalai, K. ; Velmurugan, S. ; Ravi, S. ; Kathiravan, V. and Ashokkumar, S. (2015). Green synthesis of zinc oxide nanoparticles using Moringa oleifera leaf extract and evaluation of its antimicrobial activity, Spectrochim. Acta A Mol. Biomol. Spectrosc 143: 158-164.
- Mirzaei, H. and Darroudi, M. (2017). Zinc oxide nanoparticles: biological synthesis and biomedical applications, Ceram. Int. 43: 907-914.
- Patel, V. ; Berthold, D.; Puranik, P. and Gantar, M. (2015). Screening of cyanobacteria and microalgae for their ability to synthesize silver nanoparticles with antibacterial activity, Biotechnol. Reports. 5: 112-119.
- Stan, M.; Popa, A.; Toloman, D.; Dehelean, A.; Lung, I. and Katona, G. (2015). Enhanced photocatalytic degradation properties of zinc oxide nanoparticles synthesized by using plant extracts, Mater. Sci. Semicond. Process 39: 23-29.
- Wang, X.; Lu, J.; Xu, M. and Xing, B. (2008). Sorption of pyrene by regular and nanoscaled metal oxide particles: influence of adsorbed organic matter. Environ Sci Technol. 42(19):7267-72.
- Malaikozhundan, B. (2018). Pharmaceutical Applications of Zinc Oxide Nanoparticles- A Review. Acta Scientific Pharmaceutical Sciences 2 (1): 11-12.
- Kumar, R.; Umar, A.; Kumar, G. and Nalwa, H.S. (2017). Antimicrobial properties of ZnO nanomaterials: A review. Ceramics International.43(5): 3940-3961.
- Bhumi, G.; Savithamma, N. (2014). Biological Synthesis of Zinc oxide Nanoparticles from Catharanthus roseus (L.) G. Don. Leaf extract and validation for antibacterial activity. Int. J. Drug Dev. & Res. 6 (1): 1-17.
- Hazra, C.; Kundu, D.; Chaudhari, A. and Jana, T. (2013). Biogenic synthesis, characterization, toxicity and photocatalysis of zinc sulfide nanoparticles using rhamnolipids from *Pseudomonas aeruginosa* BS01 as capping and stabilizing agent. Journal of Chemical Technology and Biotechnology. 88 (6): 1039-1048.
- Dhandapani, P.; Siddarth, A.S.; Kamalasekaran, S.; Maruthamuthu, S. and Rajagopal, G. (2014). Bio-approach: ureolytic bacteria mediated synthesis of ZnO nanocrystals on cotton fabric and evaluation of their antibacterial properties, Carbohydr. Polym 103: 448-455.
- Mitra, S.; Patra, P.; Pradhan, S.; Debnath, N.; Dey, K.K.; Sarkar, S. Chattopadhyay, D. and Goswami, A. (2015). Microwave synthesis of ZnO@mSiO<sub>2</sub> for detailed antifungal mode of action study: understanding the insights into oxidative stress, J. Colloid Interface Sci 444: 97-108.
- Abdul, H.; Sivaraj, R. (2014). Green synthesis and characterization of zinc oxide nanoparticles from Ocimum basilicum L. var. purpurascens Benth.- lamiaceae leaf extract, Mater. Lett 131: 16-18.
- Yuvakkumar, R. ; Suresh, J. ; Saravanakumar, B.; Nathanael, A. J.; Hong, S.I. and Rajendran, V. (2015). Rambutan peels promoted biomimetic synthesis of bioinspired zinc oxide nanochains for biomedical applications, Spectrochim. Acta A Mol. Biomol. Spectrosc 137: 250-258.
- Lakshmi, S. J.; Roopa, B. R. S.; Sharanagouda, H.; Ramachandra C. T. and Nidoni, U. k. (2017). A review study of zinc oxide nanoparticles synthesis from plant extracts. Green Chemistry & Technology Letters. 3(2): pp 26-37.
- Agarwal, H.; Kumar, S. V. and Rajeshkumar, S. (2017). A review on green synthesis of zinc oxide nanoparticles -An eco-friendly approach. Resource-Efficient Technologies 3 (2017) 406-413 .
- El-Batal, A. I.; Mosalam, F. M.; Ghorab, M.M.; Hanora, A. and Elbarbary, A. M.(2018). Antimicrobial, antioxidant and anticancer activities of zinc nanoparticles prepared by natural polysaccharides and gamma radiation. International Journal of Biological Macromolecules, 107(B): 2298- 2311.
- Khare, C. P. 2007. Indian medicinal plants: an illustrated dictionary. Springer Science Business Media, LLC. 812p.
- Bhandari, P.R. (2012). Garlic (*Allium sativum* L.): A review of potential therapeutic applications. Int J Green Pharm. 6:118-29.
- Hernawan, U. E. Setyawan, A. D. (2003). REVIEW: Organosulphure compound of garlic (*Allium sativum* L.) and its biological activities. Biofarmasi. 1 (2): 65-76.
- Tsiaganis, M.C.; Laskari, K.; Melissari, E. (2006). Fatty acid composition of *Allium* species lipids. Journal of Food Composition and Analysis. 19 ( 6-7): 620-627.
- Pandian, A. M. K.; Karthikeyan, C. and Rajasimman, M. (2016). Isotherm and kinetic studies on nano-sorption of Malachite Green onto *Allium sativum* mediated synthesis of silver nanoparticles. Biocatalysis and Agricultural Biotechnology. 8: 171-181.
- El-Refai, A. A.; Ghoniem, G. A.; El-Khateeb, A. Y. and Hassaan, M. M. (2018). Eco-friendly synthesis of metal nanoparticles using ginger and garlic extracts as biocompatible novel antioxidant and antimicrobial agents. J Nanostruct Chem (2018). 1-11.
- Naveen, H. K. S.; Kumar, G; Karthik, L. and Bhaskara, R.K.V. (2010). Extracellular biosynthesis of silver nanoparticles using the filamentous fungus *Penicillium sp.* Archives of Applied Science Research. 2(6): 161-167.
- Cullity, B.D. (1978). Elements of X-ray diffraction. IInd Ed. Addison Wesley. 531.
- Wei, W.; Mao, X.; Ortiz LA. And Sadoway, D.R. (2011). Oriented silver oxide nanostructures synthesized through a template-free electrochemical route. journal of Materials Chemistry. 21 (2): 432-438.
- Jobst, P.J.; Stenzel, O.; Schürmann, M.; Modsching, N.; Yulin, S.; Wilbrandt, S.; Gäbler, D.; Kaiser, N. and Tünnermann, A. (2013). Optical properties of unprotected and protected sputtered silver films: Surface morphology vs. UV/VIS reflectance. Advances in Optical Technologies. 3: 91-102.
- Ba-Abbad, M.M.; Kadhum, A.H.; Mohamad, A.B.; Takriff, M.S. and Sopian, K. (2012). Synthesis and catalytic activity of TiO<sub>2</sub> nanoparticles for photochemical oxidation of concentrated chlorophenols under direct solar radiation. International journal of electrochemical science. 7(2012): 4871-4888.
- Abu Bakar, M.R.; Nagy, Z.K. and Rielly, C.D. (2010). A combined approach of differential scanning calorimetry and hot-stage microscopy with image analysis in the investigation of sulfathiazole polymorphism. Journal of Thermal Analysis and Calorimetry, 99 (2): 609-619.
- Chekki, R. Z.; Snoussi, A., Hamrouni, I. and N. Bouzouita, (2014). Chemical composition, antibacterial and antioxidant activities of Tunisian garlic (*Allium sativum*) essential oil and ethanol extract . Mediterranean Journal of Chemistry. 3(4), 947-956.
- Park, Y.; Hong, Y.N.; Weyers, A.; Kim, Y.S. and Linhardt, R.J. (2011). Polysaccharides and phytochemicals: a natural reservoir for the green synthesis of gold and silver nanoparticles. IET Nanobiotechnology. 5 (3): 69 – 78.
- Mittal, A. K.; Chisti, Y. and Banerjee, U. C. (2013). Synthesis of metallic nanoparticles using plant extracts. Biotechnology Advances. 31(2): 346-356.
- Anita, S.; Ramachandran, T.; Koushik, C.V.; Rajendran, R.; Mahalakshmi, M. (2010). Preparation and characterization of zinc oxide nanoparticles and a study of the anti-microbial property of cotton fabric treated with the particles. JTATM 6: 1-2 .
- Gharagozlu, M. ; Baradaran, Z. and Bayati, R. (2015). A green chemical method for synthesis of ZnO nanoparticles from solid-state decomposition of Schiff-bases derived from amino acid alanine complexes, Ceram. Int. 41: 8382-8387.
- Kakil, S. A. (2014). Preparation and investigation of photodetectors based on ZnO crystals grown on silicon and porous silicon surfaces. Thesis, Degree of Master of Science in Physics College of Science-Salahaddin University/ Iraq.
- Meshram, R.S.; Suryavanshi, B.M. and Thombre, R.M. (2012). Structural and optical properties of CdS thin films obtained by spray pyrolysis. Advanced in Applied Science Research. 3: 1563-1571.